Journal of the Serbian Chemical Society
JSCS-info@shd.org.rs • www.shd.org.rs/JSCS
J. Serb. Chem. Soc. 79 (7) 881–895 (2014)
JSCS–4633
UDC 662.613.13:66.011+681.5.017:628.53
Original scientific paper

An experimental and computational investigation of the effects of temperature on soot formation mechanisms

XIAOJIE BI[1,2], MAOYU XIAO[1], XINQI QIAO[1], CHIA-FON F. LEE[2,3] and YU LIU[4]*

[1]Key Laboratory for Power Machinery and Engineering of the Ministry of Education, Shanghai Jiao Tong University, Shanghai, 200240, China, [2]Department of Mechanical Science and Engineering, University of Illinois at Urbana-Champaign, IL, 61801, USA, [3]Center for Combustion Energy and State Key Laboratory of Automotive Safety and Energy, Tsinghua University, Beijing 100084, China and [4]Key Laboratory of Automobile Dynamic Simulation, Jilin University, Changchun, Jilin, 130012, China

(Received 14 June, revised 2 November, accepted 4 November 2013)

Abstract: Effects of the initial ambient temperature on combustion and soot emission characteristics of diesel fuel were investigated through experiments conducted in an optical constant volume chamber and simulation using a phenomenological soot model. Four different initial ambient temperatures were adopted in this research: 1000, 900, 800 and 700 K. In order to obtain a better prediction of soot behavior, the phenomenological soot model was revised to take into account the feedback of soot oxidation on the soot number density and good agreement was observed in the comparison of soot measurement and prediction. The results indicated that the ignition delay was prolonged with decreasing initial ambient temperature. The heat release rate demonstrated the transition from mixing controlled combustion at high ambient temperatures to the premixed combustion mode at low ambient temperatures. At lower ambient temperatures, soot formation and the oxidation mechanism were both suppressed. However, the soot mass concentration was finally reduced with decreasing initial ambient temperature. Although the drop in ambient temperature did not cool the mean in-cylinder temperature during the combustion, it did shrink the total area of local high equivalence ratios, in which soot usually is rapidly generated. At an initial ambient temperature of 700 K, soot emissions were almost negligible, which indicates that sootless combustion might be achieved under super low initial temperature operation conditions.

Keywords: soot emission; constant volume chamber; phenomenological soot model; multi-dimensional simulation.

* Corresponding author. E-mail: xiaojie2163@hotmail.com
doi: 10.2298/JSC130614125B

INTRODUCTION

Soot, a major component of particulate matter (PM), is one of the key air pollutants emitted by diesel engines.[1] Previous research proved that soot nuclei with a radius between 0.1 and 0.5 μm are able to deposit directly in the lung and result in serious health issues.[2] Therefore, there is a global trend to enforce more stringent regulations for this air pollutant. In addition to the emissions challenge, soot formation in diesel engines can also influence the engine performance and have feedback effects on in-cylinder combustion and emission characteristics. Soot, once present within a flame, plays an important role in radiative heat transfer:[3,4] soot produces broadband incandescent radiation, which typically dominates over narrow-band radiation from intermolecular processes. Therefore, soot appearance within a flame would enhance the flame emissivity and hence increase radiative heat loss. The combustion efficiency then tends to decrease. In addition, a lower flame temperature, owing to the larger radiative heat transfer through soot nuclei, will in turn suppress NOx formation.[5]

Although it is essential to clarify soot formation and oxidation mechanisms, the understanding about the factors affecting soot particles is still limited. Most research was conducted under near-atmospheric conditions.[6–9] However, combustion and soot formation in diesel fuel jets under a high-temperature and high-pressure environment is far removed from atmospheric conditions. Laser diagnostics measurements conducted in high-temperature, high-pressure combustion vessels[10–14] are typical tools capable of yielding detailed measurements of soot processes under diesel-like operation conditions. Overall, soot in diesel fuel jets begins to be generated shortly after auto-ignition and lasts throughout all the transient premixed phase and the ensuing mixing-controlled phase of combustion.[15–17]

There is a wide range of parameters, such as temperature, pressure, equivalence ratio, fuel composition and structure, as well as engine design and operation parameters, that are involved in soot evolution, among which temperature plays the most important role.[1] Soot and temperature have an inherent coupled dependence: temperature depends on soot concentration due to heat transfer through radiation and soot depends on temperature due to the chemical and physical processes controlled by temperature. Therefore, a detailed understanding of soot must depend on an in-depth analysis of temperature. In a constant volume chamber, an increase in soot generation with increasing temperature was observed by Pickett and Siebers,[18] due to increasing rates of the soot formation reaction. In shock-tube measurements, Graham *et al.*[19] found that soot volume fraction exhibited a bell-shaped behavior as a function of temperature in the pyrolysis of aromatics. This behavior was also reported by Frenklach *et al.*[20] within the flame of non-aromatic fuels, when the soot volume fraction initially increased and then decreased with increasing temperature. The temperature under which the soot

yield reaches its peak was found to vary widely over various configurations.[21,22] Additionally, multi-dimensional simulation is essential for the interpretation of experimental discoveries in order to obtain an in-depth understanding about soot evolution. For decades, many contributions have been made to explore suitable models to describe soot formation and oxidation in a turbulent non-premixed flame. Moss *et al.*[23] developed a two-step soot model using vapor-phase diesel fuel as the soot precursor. The first step is a soot mass fraction equation, including surface growth and nucleation and the second is an equation of soot number density, using nucleation and coagulation as the source and sink terms. Tesner *et al.*[24] introduced a general precursor species and linked the precursor species with soot particles through a coagulation process. Sequentially, Surovikin *et al.*[25] improved the Tesner model[24] and adopted surface growth to be the conversion pathway from the soot precursor to soot nuclei, once the diameter of precursor species was larger than a critical diameter. Based on the previous work, Leung *et al.*[26] adopted acetylene as the precursor species and further considered surface growth reactions between soot and acetylene. Subsequently, Fusco *et al.*[27] developed an eight-step phenomenological soot model by introducing oxidative reactions of acetylene and precursor species to avoid an overestimation of their concentrations. Tao *et al.*[22] improved the Fusco model[27] by including the involvement OH radicals in a soot oxidation mechanism through the Neoh OH-related oxidation model[28] in a newly revised phenomenological soot model.[22]

Some may argue that this phenomenological soot model is too simplified to describe soot evolution in a turbulent non-premixed flame since it is a rather complex process, involving the interaction of chemical kinetics, heat and mass transfer as well as fluid flow and a description of pre-particle chemistry. However, the soot formation and oxidation process under diesel-like conditions were elusive, especially gas-phase kinetics from diesel fuel to soot nuclei were then uncertain subjects.[29] At present, a detailed chemistry soot model is well accepted as the most accurate model for the prediction of soot behavior because all known reactions and species relevant to soot formation and oxidation were taken into account.[30–33] However, a detailed representation of soot chemical reactions needs the interactions between the detailed chemistry and turbulent mixing on a sub-grid level to be solved. By doing this, the model is super demanding in terms of computational time and rather impractical. Additionally, accurate predictions of soot evolution are extremely sensitive not only to the soot model itself, but also to the other models that are applied to describe the complex processes of spray and combustion processes, such as the turbulence model, the spray model and the evaporation model. These existing uncertainties in these models could essentially eliminate the advantages of using a detailed kinetic treatment of soot formation. Therefore, the choice of a simplified phenomenological soot model is the combination result of computation efficiency and acceptable accuracy.

The objective of the current study was to explore the temperature effects on soot formation and oxidation of diesel fuel under diesel-like operation conditions. Detailed analysis of the in-cylinder pressure, heat release rate and time related soot behavior was provided to expand the understanding of the coupled dependence of temperature and soot nuclei. In order to interpret the new experimental findings, a phenomenological soot model was revised and applied to predicted soot behavior under the same operational conditions. Time related traces and spatial distributions of soot relevant species, such as acetylene, soot precursor species, OH radicals and soot number density were predicted as well.

EXPERIMENTAL

Experimental apparatus

The experiments were conducted in an optical-accessible constant volume chamber with a bore of 110 mm and a height of 65 mm. The chamber was designed to imitate spray and combustion processes in compressed ignition engines with a maximum operating pressure of 18 MPa. The chamber together with a liquid spray scattering, combustion flame and soot formation measurement setup is shown schematically in Fig. 1. In order to pass laser beams and take photographs, a fused silica (Dynasil 1100) end window, 130 mm in diameter, 60 mm thick and with high UV transmittance down to 190 nm, was installed opposite to the injector.

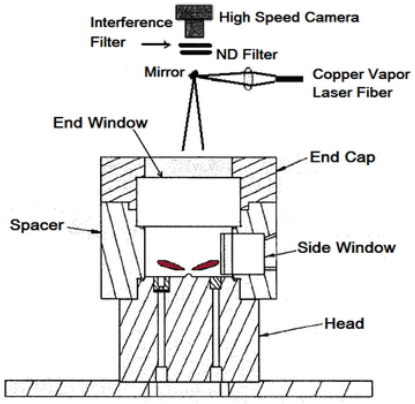

Fig. 1. A schematic presentation of the constant volume chamber.

Details of the apparatus are given in the Supplementary material to this paper.

Experimental methods

In these experiments, the forward illumination light extinction (FILE) method developed by Xu and Lee[34] was used as the soot diagnostic technology. This method was able to provide two dimensional time-resolved quantitative soot measurements. As shown in Fig. 1, in the FILE method, the light source and the camera are placed on the same side of the flame through the same window. By doing this, only one window with a light diffuser is required in the forward-illumination setup, as shown in Fig. S-1 of the Supplementary material. Compared to the back illumination light-extinction method, in which two aligned windows are

required, the FILE technique was easier to operate. The light diffuser set behind the flame was to ensure sufficient reflected light that could be collected by the camera.

Details of the extinction measurements and the subsequent calculations are given in the Supplementary material.

Experimental procedure

Initially, a premixed, combustible-gas mixture of acetylene (C_2H_2), air and nitrogen was filled into the test chamber. After the mixture had been ignited by spark plugs, a high-temperature, high-pressure environment modeling typical diesel in a cylinder environment with the piston at TDC was created in the test chamber. Due to its flammability and low window contamination, acetylene, with unity C/H ratio, was adopted here as the pilot combustion gas. Thus, the density of the filling mixture can be determined by the chemical reaction as:

$$4C_2H_2 + (10 + \zeta)O_2 + 65N_2 \rightarrow 8CO_2 + 4H_2O + \zeta O_2 + 65N_2 \quad (1)$$

where ζ denotes the amount of excess oxygen, which was used to simulate the ambient oxygen concentration for diesel compressed ignition combustion. After the acetylene had been completely consumed, the ambient air contained 21 % oxygen, 66.7 % nitrogen, 8.2 % carbon dioxide and 4.1 % water vapor by volume. The density of the mixture for post-combustion was 14.8 kg m^{-3}, which mimics the operation conditions without the EGR rate of realistic diesel engines. In addition, the vessel pressure slowly decreases due to heat transfer through the vessel walls. When the desired pressure was achieved the injection signal triggered the HEUI injector and the high-speed camera simultaneously, and diesel fuel was injected into the cylinder and the camera began to record the whole injection, auto-ignition and combustion processes.

In this study, four different ambient temperatures were investigated:700, 800, 900 and 1000 K, covering both low-temperature and conventional high-temperature combustion modes in diesel engines, *i.e*., initial temperatures of 700 to 800 K present low temperature low load combustion while an initial temperature of 1000 K presents typical high temperature higher load combustion. The test fuel in these experiments was European low sulfur diesel fuel.

Simulation models

In order to obtain insight into the formation and oxidation mechanisms of soot particles, a phenomenological soot model was adopted and revised to simulate compressed ignition combustion and soot emission behavior at initial ambient temperatures of 700 to 1000 K. The soot model in the present paper restrained the main feature of the phenomenological soot model developed by Tao *et al*.,[22] but improved the governing differential equation of soot number density by taking into account the effects of soot oxidation. A schematic presentation of the revised phenomenological soot model is shown in Fig. 2, from which it can be seen that the Phenomenological soot model has nine main steps.

Complete descriptions of the models considered in this study are given in the Supplementary material.

RESULTS AND DISCUSSION

Analysis of the combustion characteristics

The measured in-cylinder pressure and heat release rate under ambient temperatures of 700, 800, 900 and 1000 K are presented in Fig. 3. Since the chamber volume is constant, the in-cylinder pressure is directly proportional to temperature and the higher the initial temperature, the higher is the initial pressure. In

order to avoid the influence of the initial in-cylinder pressure, all initial pressures were set to zero and hence the pressures shown in the Fig. 3 are relative pressures, which are actually the increase of pressure caused by heat released from the diffusion-dominated combustion.

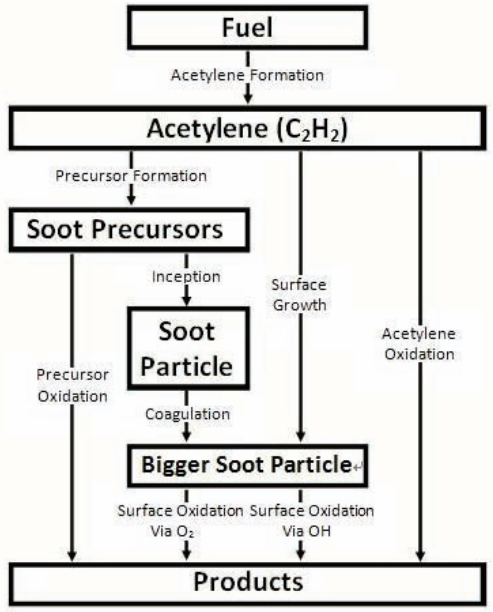

Fig. 2. Structure of the nine-step phenomenological soot model.

As shown in Fig. 3, the ignition delay became longer with decreasing initial temperature from 1000 to 700 K. The threshold of combustion here is defined as the time when a sudden increase in the heat release rate first appeared. Based on the theory of chemical kinetics, the ambient temperature is the most essential parameter in the determination of chemical reaction rates. With decreasing ambient temperature, the effective coagulation frequency between reactants tends to

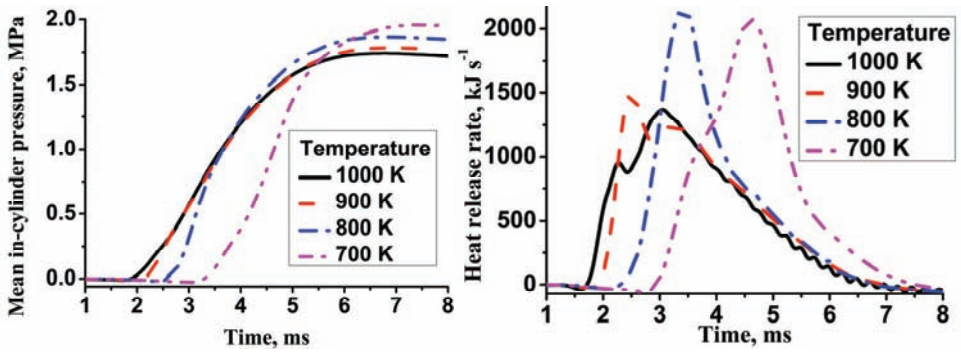

Fig. 3. In-cylinder pressure and heat release rate determined using the phenomenological soot model.

decrease and the reaction rates of all chemical reactions are retarded. Therefore, a milder and slower heat release rate could be expected for pre-flame reactions. More time was required to achieve self-ignition and the ignition delay was longer.

On the other hand, premixed combustion becomes a more and more important part of the whole combustion process with decreasing initial ambient temperature. When the ambient temperature was as high as 1000 K, there were two peaks in the rate of heat release trace, indicating premixed and diffusion combustion, respectively. On dropping the ambient temperature to 900 K, a higher premixed combustion peak as well as a lower diffusion combustion peak than at 1000 K initial ambient temperature were found in Fig. 3. When the initial ambient temperature was further decreased to 800 K, only one peak was observed in heat release rate trace, which illustrated that premixed combustion was the absolutely dominant combustion mode under this operation condition and the combustion pressure was even higher than that under 900 K initial ambient temperature. At 700 K initial ambient temperature, the heat release rate retained a one-peak characteristic and the highest combustion pressure was found, Fig. 3, evidencing the highest combustion efficiency. As discussed above, the ignition delay became longer with decreasing initial ambient temperature. A longer ignition delay gives more time for the fuel and fresh air to mix, resulting in the formation of a larger premixed charge before self-ignition and hence a stronger premixed combustion would occur on ignition of the diesel. Hence, the peak of the premixed combustion was higher at the lower initial ambient temperature. The speed of premixed flames is dependent on the chemical reaction rates, while the speed of diffusion flames is determined by the diffusion speed. Since chemical reaction rates are much faster than diffusion speed, the combustion duration was much shorter for premixed dominated combustion for initial ambient temperature of 800 and 700 K than that occurring with initial ambient temperatures of 900 and 1000 K. The heat loss was decreased due to the shorter combustion duration at lower initial ambient temperatures. In the experiments, the total fuel mass was kept constant, which indicated a constant energy input for all operation conditions. With a lower heat loss, the combustion efficiency was higher with decreasing initial ambient temperature and became the highest at 700 K initial ambient temperature; thus, the highest-pressure peak was observed at 700 K initial ambient temperature, as shown in Fig. 3.

Soot behavior analysis

The time related total soot mass concentrations at initial ambient temperatures of 700 to 1000 K are shown in Fig. 4. In order to avoid the effects of the amount of fuel injected on the soot generation, the unit $\mu g\ g_{fuel}^{-1}$ was adopted here, which was defined as the total mass of soot in the chamber over the total mass of injected diesel fuel. In Fig. 4, the soot mass exhibited “bell-shaped”

characteristics regardless of the initial temperature, *i.e.*, the amount of soot initially increased rapidly to achieve maxima values and then decreased to zero thereafter. Similar results were also reported in previous studies.[21,22,27] The threshold of soot mass formation was gradually delayed on decreasing the initial ambient temperature from 1000 to 700 K and the duration of the delay became longer in the order 900 to 1000 K, 800 to 900 K and finally 700 to 800 K. As discussed above, the auto ignition delay was longer at lower initial ambient temperatures. Since soot particles are the incomplete products of compressed ignition combustion, they followed the same characteristics of combustion and their appearance occurred later with decreasing initial temperature from 1000 to 700 K.

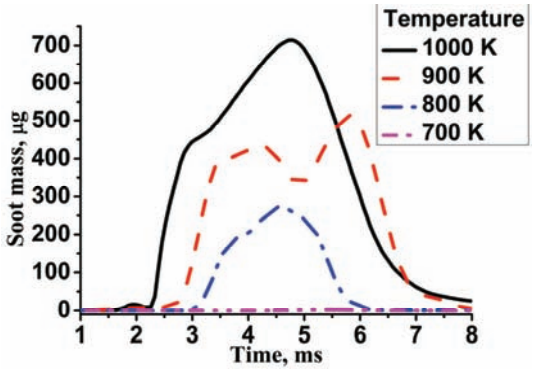

Fig. 4. Soot mass generated by 1 g of fuel for initial temperatures of 700, 800, 900 and 1000 K.

The later appearance of soot also demonstrates the reduced tendency of sooting of diesel fuel at lower initial ambient temperatures. Therefore, the total soot mass increased with increasing ambient temperature, which emphasized the importance of intake temperature cooling and its beneficial effects on mitigating soot formation. The soot emissions here were the combined results of soot formation and soot oxidation. Under conditions of higher ambient temperatures, weaker premixed combustion was observed, Fig. 3, so less entrainment of ambient air would result in higher fuel richness within the diesel fuel jet, higher soot formation rates at the early stage of combustion and finally higher soot mass concentration, as shown in Fig. 4.

Validation of phenomenological soot model

Comparisons between the measured and predicted soot behavior using the revised phenomenological soot model for initial temperatures of 700, 800, 900 and 1000 K are illustrated in Fig. 5, which shows that the overall soot traces predicted by revised phenomenological soot model were in good agreement with the measurements. Therefore, it is reasonable to believe that phenomenological soot model is able to reproduce successfully the soot formation and oxidation

processes of diesel fuel and its prediction for relevant intermediate species, such as acetylene, soot precursor species and OH radicals.

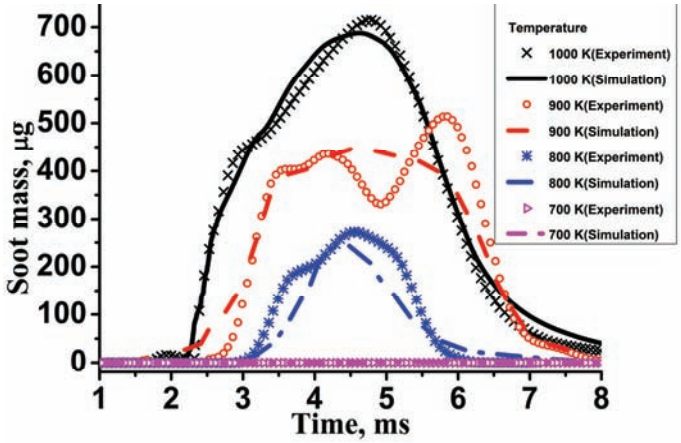

Fig. 5 Comparison of the measured and predicted soot mass generated by 1 g of fuel for initial temperatures of 700, 800, 900 and 1000 K.

Predicted traces of soot relevant species

The temporal mass concentrations of C_2H_2, soot precursors, OH radicals and soot number predicted by the revised phenomenological soot model for initial ambient temperatures of 700 to 1000 K are shown in Fig. 6, from which it can be seen that all traces shared the same "bell-shaped" characteristics as the soot mass concentration. Comparing Fig. 6 to Fig. 5, it is evident that there were no significant differences between the soot mass and the amount of soot, which indicated that the initial temperature had negligible effects on the mean particle diameter of the soot in the constant volume chamber.

As shown in Fig. 6, the thresholds for soot relevant species were also retarded with decreasing initial ambient temperature from 1000 to 700 K. Acetylene and soot precursor species are typical intermediate species involved in diesel compressed ignition combustion. The initial temperature is the most essential parameter determining the rates of pre-flame reactions. In Fig. 4, the longest ignition delay was observed at the lowest initial temperature, when the lowest reaction rates for the pre-flame reactions were also observed. As a result, lower formation rates of acetylene and soot precursor species could be expected in the early stages of combustion and delayed appearances of acetylene and soot precursor species were found at the lowest initial temperature, as shown in Fig. 6.

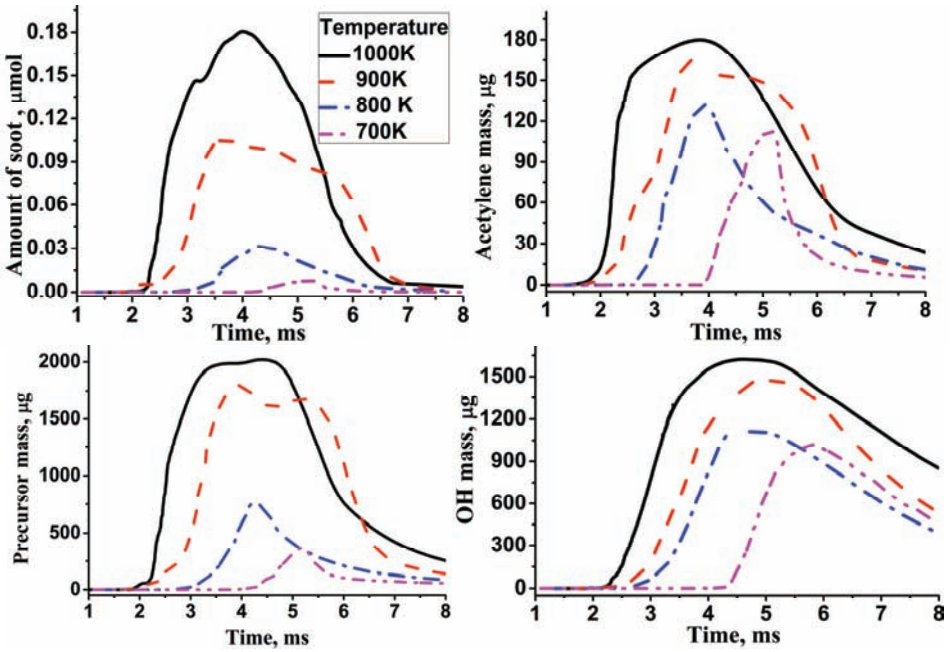

Fig. 6. Soot mass, amount of soot, mass of C_2H_2, soot precursor and OH generated by 1 g of fuel for initial temperatures from 700 to 1000 K.

In Fig. 6, the continuous decrease in the maximum mass concentrations of species relevant for soot formation and oxidation mechanisms, such as acetylene, soot precursor species and OH radicals, indicated that both soot formation and oxidation reactions were strongly suppressed by the reduced initial ambient temperature. However, a lower total soot mass concentration with the decreasing ambient temperatures was previously proved. Therefore, it is reasonable to believe that the soot formation mechanism played a leading role in dominating the behaviors of soot when the initial ambient temperature was decreased.

Below an initial ambient temperature of 800 K, a suddenly sharp drop appeared in the mass concentration of soot precursor species. In the new proposed model, there are one formation pathway and mainly two consumption pathways directly linked to the mass concentration of the soot precursor species: generation from an acetylene-rich pool, condensation to form soot nuclei and directly oxidation to CO_2 and H_2O. As shown in Fig. 6, the mass concentration of OH radicals continued to decrease with decreasing initial ambient temperature, which led to a lower oxidation rate of the soot precursor species. At the same time, a lower rate of soot formation from soot precursor species was also proved previously at lower initial ambient temperatures. Therefore, the reason for the lower peak of the precursor mass concentration at lower initial ambient temperatures should only be the lower formation rate of soot precursor species from

acetylene. The decrease of initial temperature not only suppressed the formation rate of soot particles but also restrained the formation mechanism of the intermediate species. When the initial temperature was 700 K, the mass concentration of soot precursor species was almost zero and a super low level of soot emissions (near zero), as presented in Fig. 5. Since soot emissions exhibited a continuous decrease with decreasing initial ambient temperature, smokeless combustion might be achieved after a further reduction in the initial ambient temperature.

Predicted spatial distributions of soot emissions and relevant species

The spatial distributions of the mean in-cylinder temperature, equivalence ratio, amount and mass of soot nuclei, acetylene, soot precursor species as well as OH radicals are presented in Fig. S-2, Supplementary material, for initial ambient temperatures from 700 to 1000 K at 4.5 ms, when the mass concentrations of soot emissions achieved their peaks under 800, 900 and 1000 K initial ambient temperatures.

Under the constant initial ambient temperature, the diesel fuel, acetylene, precursor species, soot particles and OH radicals were all detected within the high temperature area, which determined that there should be a switch temperature above which soot formation and oxidation reactions could be reactivated. Compared to the distributions of acetylene and the soot precursor species, the distributions of the OH radical, which is the representative reactant involved in soot oxidation reactions, had shapes more similar to those of the temperature distributions. Thus, the oxidation mechanisms of soot particles were highly dependent on the ambient temperature.

For initial temperatures from 1000 to 700 K, the local highest mean in-cylinder temperature did not show an obvious decrease under the operation condition with the lower initial ambient temperatures, as shown in Fig. S-2. Furthermore, the overall temperature was even higher at an initial ambient temperature 800 K than that at initial ambient temperatures of 900 and 1000 K. At 700 K ambient temperature, the region of high combustion temperatures started to shrink. Since a continuous drop in the peaks of the total mass concentrations of soot were observed in Fig. 5, the decrease in initial ambient temperature was not the direct reason for the reduction of soot emissions.

The equivalence ratio is defined as the local fuel/oxidizer mass ratio divided by the stoichiometric fuel/oxidizer mass ratio. When the initial temperature dropped from 1000 to 800 K, the maximum equivalence ratio value of local fuel-rich reaction zone did not decrease very much. However, the area of local fuel-rich zone did decrease gradually. Similar results were also observed in the mass concentration distributions of acetylene and the soot precursor species for ambient temperatures from 800 to 1000 K, the maximum mass density of acetylene and the soot precursor species at the lowest initial temperature maintained the

same level as those at the higher initial ambient temperatures, which was evidenced by the almost same red color in Fig. S-2. However, the area of the local rich reaction zone of acetylene and the soot precursor species shrank a lot at lower initial ambient temperatures, especially at an initial ambient temperature of 800 K. Therefore, the suppressed soot formation mechanism at the lower initial temperature conditions should be directly caused by the reduced area of the local diesel-rich reaction zones.

Comparing spatial distributions in Fig. S-2, it is clearly noticeable that the soot mass distributions did not duplicate the distributions of the equivalence ratios. However, it looked more like the distributions of soot precursor species. This result revealed that soot precursors were the species to determine the locations where soot particles existed. The soot mass density was the result of combining both the effects of acetylene and the soot precursor species.

When initial temperature dropped to as low as 700 K, the highest local equivalence ratio should be below 2, since all the red and yellow color in equivalence ratio distribution faded away. As shown in Fig. 5, the soot mass concentration was negligible under this condition. Furthermore, it is very clear that the mass concentration became larger in the order of soot particles, soot precursor species and acetylene, which means gas-phase species, including acetylene and soot precursor species, had a wider region of equivalence ratio for their formation. Similar conclusions were also reached in an investigation of Kitamura *et al.*,[35] who modeled the equivalence ratio and temperature dependence of soot formation for paraffinic hydrocarbons, aromatic hydrocarbons and oxygenated hydrocarbons using a detailed soot kinetic model. In their research, the critical equivalence ratio of *n*-heptane was around 2, indicating that soot is not formed at equivalence ratios below 2, regardless of the temperature. Moreover, they found that the acetylene formation region was distributed over a wider equivalence ratio region than the sooting region. These results were consistent with the present observations. Since soot mass concentration decreased with decreasing initial temperature, sootless combustion could be expected when the initial temperature is below 700 K.

CONCLUSIONS

Experiments were conducted in an optical constant volume chamber to explore combustion and soot emission characteristics under different initial ambient temperatures, 700, 800, 900 and 1000 K. To aid interpretation of the experimental results, a phenomenological soot model was revised and the revision applied to predict soot behavior under the same operation conditions as in the experiments. Qualitatively, a comparison of soot measurements and the predictions from the phenomenological soot model were given to validate the revised soot model. Detailed analysis about soot relevant species, such as acetylene, pre-

cursor species and OH radicals was also presented to reveal the responsible factor that contributed to the reduction of soot emissions with decreasing initial ambient temperature. The main conclusions are as follows:

The heat release rates demonstrate the transition from mixing controlled combustion at 1000 and 900 K to premixed combustion dominant at 800 and 700 K. A longer ignition delay was also observed at lower initial ambient temperature conditions. The in-cylinder pressure traces proved that the combustion efficiency became higher when initial ambient temperature was decreased from 1000 to 700 K.

Similar to the combustion characteristics, a delayed appearance of soot emissions was found at lower initial ambient temperatures. Moreover, the total soot mass increased with increasing ambient temperatures. At an initial ambient temperature of 700 K, the soot emissions were almost negligible, which indicates that sootless combustion might be achieved under low initial temperature conditions.

All species relevant to soot formation and the oxidation mechanism presented a delayed threshold of increase in soot formation as the initial ambient temperature decreased from 1000 to 700 K. The mass concentrations of acetylene, soot precursor species and OH radicals decreased with decreasing temperature. The slower formation and oxidation reaction rates at lower initial temperature indicated that the soot formation mechanism dominated the soot behavior under various initial ambient temperatures.

The effects of the initial ambient temperature on the mean in-cylinder temperature were unperceivable. However, variation in the initial ambient temperature could strongly affect the distribution of the equivalence ratio within the whole test chamber. The total area of local high equivalence ratio shrunk at lower initial ambient temperature revealed a reduced sooting tendency; hence, lower soot emissions were detected with decreasing initial ambient temperature. At an initial ambient temperature of 700 K, the equivalence ratio was under the value of 2. Soot was not formed at equivalence ratios below 2, regardless of temperature.

SUPPLEMENTARY MATERIAL

Details of the apparatus, information on the measurement and subsequent calculation of extinction values, model description, a list of employed symbols and figures of spatial in-cylinder phenomena are available electronically at http://www.shd.org.rs/JSCS/, or from the corresponding author on request.

ИЗВОД

ЕКСПЕРИМЕНТАЛНО И РАЧУНАРСКО ИСПИТИВАЊЕ УТИЦАЈА ТЕМПЕРАТУРЕ НА МЕХАНИЗМЕ СТВАРАЊА ЧАЂИ

XIAOJIE BI[1,2], MAOYU XIAO[1], XINQI QIAO[1], CHIA-FON F. LEE[2,3] и YU LIU[4]

[1]Key Laboratory for power machinery and Engineering of Ministry of Education, Shanghai Jiao Tong University, Shanghai, 200240, China, [2]Department of Mechanical Science and Engineering, University of Illinois at Urbana-Champaign, IL, 61801, United States, [3]Center for Combustion Energy and State Key Laboratory of Automotive Safety and Energy, Tsinghua University, Beijing 100084, China и [4]Key Laboratory of automobile dynamic simulation, Jilin University, Changchun, Jilin, 130012, China

Испитани су утицаји почетних температура средине на карактеристике сагоревања дизел горива и емисије чађи применом експеримента спроведених у оптичкој комори сталне запремине и помоћу симулације која користи феноменолошки модел чађи. У истраживањима су разматране четири почетне температуре средине: 1000, 900, 800 и 700 K. Како би се добило боље предвиђање понашања чађи ревидиран је феноменолошки модел чађи како би се узео у обзир повратни утицај оксидације чађи на густину расподеле чађи, при чему је добијено добро слагање између мерења и предвиђања. Резултати су показали да је одлагање паљења везано са смањењем почетне температуре средине. Интезитет ослобађања топлоте демонстрира прелаз од дифузионог сагоревања на високој температури до предмешаног сагоревања на ниској температури. На нижој температури су потиснути процеси оксидације и формирања чађи. Ипак, на крају је масена концентрација чађи смањена са смањењем почетне температуре средине. Иако пад у температури средине није охладио главни улазни вод за време сагоревања, он није смањио високе вредности локалног еквивалентног односа гориво/ваздух, у којој се чађ по правилу брзо стварала. На почетној температури средине од 700 K, емисије чађи су биле скоро занемарљиве, што указује на то да сагоревање без чађи може бити остварено у условима изузетно ниских почетних радних температура.

(Примљено 14. јуна, ревидирано 2. новембра, прихваћено 4 новембра 2013)

REFERENCES

1. D. R. Tree, K. I. Svensson, *Prog. Energ. Combust. Sci.* **33** (2007) 272
2. V. Lépicier, M. Chiron, R. Joumard, *Environ. Impact Assess. Rev.* **38** (2013) 35
3. K. Boulouchos, M. K. Eberle, B. Ineichen, C. Klukowski, *Heat Transfer in Diesel Engines*, SAE Technical Paper 890573, 1989, doi:10.4271/890573
4. P. Flynn, M. Mizusawa, O. A. Uyehara, P. S. Myers, *SAE Trans.* **81** (1972) 95
5. B. J. Alder, L. K. Tseng, N. M. Laurendeau, J. P. Gore, *Combust. Sci. Technol.* **152** (2000) 167
6. F. Douce, N. Djebaïli-Chaumeix, C. E. Paillard, C. Clinard, J. N. Rouzaud, *Proc. Combust. Inst.* **28** (2000) 2523
7. A. V. Eremin, *Prog. Energ. Combust. Sci.* **38** (2012) 1
8. O. Mathieu, N. Djebaïli-Chaumeix, C. E. Paillard, F. Douce, *Combust. Flame* **156** (2009) 1576
9. N. Ohashi, K. Ishii, A. Teraji, M. Kubo, *Nihon Kikai Gakkai Ronbunshu, B. Hen, Trans. Jpn. Soc. Mech. Eng., B* **75** (2009) 2520
10. Á. Díez, H. Zhao, T. Carrozzo, A. E. Catania, E. Spessa, *P. I. Mech. Eng., D – J. Aut. Eng.* **226** (2012) 684
11. Y. Wu, R. Huang, C. F. Lee, C. Huang, *P. I. Mech. Eng., D – J. Aut. Eng.* **226** (2012) 372
12. H. Liu, X. Bi, M. Huo, C. F. F. Lee, M. Yao, *Energy Fuels* **26** (2012) 1900

13. H. Liu, C. F. Lee, M. Huo, M. Yao, *Energy Fuels* **25** (2011) 1837
14. H. Liu, C. F. F. Lee, M. Huo, M. Yao, *Energy Fuels* **25** (2011) 3192
15. D. H. Qi, H. Chen, L. M. Geng, Y. Z. Bian, *Energy Convers. Manage.* **51** (2010) 2985
16. D. H. Qi, H. Chen, L. M. Geng, Y. Z. Bian, X. C. Ren, *Appl. Energy* **87** (2010) 1679
17. D. H. Qi, L. M. Geng, H. Chen, Y. Z. Bian, J. Liu, X. C. Ren, *Renew. Energy* **34** (2009) 2706
18. L. Pickett, J. López, *Jet-Wall Interaction Effects on Diesel Combustion and Soot Formation*, SAE Technical Paper 2005-01-0921, 2005, doi: 10.4271/2005-01-0921
19. S. Graham, J. Homer, J. Rosenfeld, *Proc. Roy. Soc. London* **344** (1975) 259
20. M. Frenklach, S. Taki, M. B. Durgaprasad, R. A. Matula, *Combust. Flame* **54** (1983) 81
21. F. Tao, D. E. Foster, R. D. Reitz, *Proc. Combust. Inst.* **31** (2007) 2991
22. F. Tao, R. D. Reitz, D. E. Foster, Y. Liu, *Int. J. Therm. Sci.* **48** (2009) 1223
23. J. B. Moss, C. D. Stewart, K. J. Syed, *Proc. Combust. Inst.* **22** (1989) 413
24. P. A. Tesner, T. D. Smegiriova, V. G. Knorre, *Combust. Flame* **17** (1971) 253
25. V. F. Surovikin, *Solid Fuel Chem.* **10** (1976) 92
26. K. M. Leung, R. P. Lindstedt, W. P. Jones, *Combust. Flame* **87** (1991) 289
27. A. Fusco, A. L. Knox-Kelecy, D. E. Foster, in *Proceedings of the 3rd International Symposium on Diagnostics and Modeling of Combustion in Internal Combustion Engines*, COMODIA 94, Yokohama, Japan, 1994, p. 571
28. K. G. Neoh, J. B. Howard, A. F. Sarofim, *Proc. Combust. Inst.* **20** (1985) 951
29. A. E. Karataş, O. L. Gülder, *Prog. Energ. Combust. Sci.* **38** (2012) 818
30. F. Tao, V. I. Golovitchev, J. Chomiak, *Combust. Flame* **136** (2004) 270
31. Y. Ren, X. G. Li, *P. I. Mech. Eng., D – J. Aut. Eng.* **225** (2011) 531
32. M. Yao, Z. Zheng, *P. I. Mech. Eng., D – J. Aut. Eng.* **220** (2006) 991
33. H. Zhao, Z. Peng, N. Ladommatos, *P. I. Mech. Eng., D – J. Aut. Eng.* **215** (2001) 1297
34. Y. Xu, C. F. Lee, *Appl. Optics* **45** (2006) 2046
35. T. Kitamura, T. Ito, J. Senda, H. Fujimoto, *Int. J. Engine Res.* **3** (2002) 223.